Available online at www.sciencedirect.com

SciVerse ScienceDirect

Journal of the European Ceramic Society 32 (2012) 1915–1923

www.elsevier.com/locate/jeurceramsoc

Diamond-ceramics composites—New materials for a wide range of challenging applications

Mathias Herrmann [a,*], Björn Matthey [a], Sören Höhn [a], Isabel Kinski [a], David Rafaja [b], Alexander Michaelis [a]

[a] *Fraunhofer Institute for Ceramic Technologies and Systems, Dresden, Germany*
[b] *Institute of Material Science, TU Bergakademie Freiberg, Germany*

Available online 1 December 2011

Abstract

Materials with enhanced wear resistance are of great interest for modern industry. The different ways of producing superhard ceramic materials are shortly reviewed. In detail, the preparation of diamond–silicon carbide composites by reactive infiltration of diamond preforms with liquid silicon at ambient pressure is investigated. In addition to homogeneous SiC/diamond materials with nearly 50 vol.% of diamond layered composites were also prepared. The microstructures of the materials prepared under different infiltration conditions were analyzed using X-ray diffraction, electron microscopy, electron back-scatter diffraction (EBSD) and Raman spectroscopy. The properties of the materials depend strongly on the formation of graphite interlayers at the boundary between SiC and diamond. Hardness of 47 GPa was reached for materials where the formation of the interlayer was prevented.

Keywords: Sintering; SiC; Hardness; Diamond; Composites

1. Introduction

Materials with enhanced wear resistance are of great interest for modern industry because they allow for a significant increase in lifetime, for meeting severe operating conditions or even for new applications and processes.[1,2,6] Although they exhibit complex wear processes with overlapping chemical, thermal and mechanical processes, most wear-resistant materials have high hardness and fracture toughness.[1] Therefore, it is not surprising that most of them belong to the group of superhard materials based on diamond or cubic boron nitride. The disadvantage of these materials is the need for high pressures and temperatures for their production that implies high costs and certain geometry restrictions. Hence, an intensive search for new cost-effective technologies is currently taking place.[1] There are two principal ways of producing superhard ceramic materials for advanced wear applications: (i) covering the ceramics with superhard coatings and (ii) production of superhard composite materials via sintering.

The diamond coatings of ceramics having the typical thickness of 5–20 μm are a suitable alternative when primarily the surface of the material (tool/component) has to be protected against wear. For such applications, silicon nitride and silicon carbide ceramics coated by chemically vapour deposited (CVD) diamond were recently successfully developed.[2,3] These are highly wear-resistant materials with low-friction that are appropriate for a wide range of applications, e.g. cutting tools, drawing dies and face seals.[2,3] The latter was introduced on the market under the name DiamondFaces®.[3,4] The wear resistance and the performance of such a component strongly depend on the stability of the interface between the ceramic substrate and the diamond coating. In the meantime, the coating technology was tailored particularly to achieve high-quality components with high reliability of the interfaces.[3,4] For certain applications, in which the overloading of the interface or a higher amount of wear occurs, the CVD coatings are not the best choice, and bulk superhard materials are preferred. The preparation of the bulk superhard materials involves a sintering process. The sintering requires mass transport through a diffusion process, which is significantly accelerated at high temperatures or via transport in a liquid phase. However, if working with metastable phases like diamond or c-BN, the use of high temperatures must be

* Corresponding author. Tel.: +49 351 255 3600; fax: +49 351 255 3600.
E-mail address: Mathias.Herrmann@ikts.fraunhofer.de (M. Herrmann).

0955-2219/$ – see front matter © 2011 Elsevier Ltd. All rights reserved.
doi:10.1016/j.jeurceramsoc.2011.11.005

accompanied by high pressures in order to prevent the transformation of the superhard metastable phases to the stable modifications, which usually have a substantially lower hardness. Regarding the reduction of the production costs, the development of a new technology for fabrication of compact superhard materials without application of high pressure is a challenging task.

A possible approach of the manufacturing without application of high pressure has to take place under conditions under which a solution of the metastable hard component (e.g. diamond and cBN) and precipitation of the stable phase is suppressed. This can be achieved in composites with a high content of the hard phase that is strongly bonded in a matrix. However, the sintering of a matrix with rigid inclusions results in a strong reduction of the sintering activity due to the stresses that are generated in the matrix by the rigid inclusions.[5] These stresses are especially strong near or above the percolation threshold and result in local residual porosity.[5] The stresses can be reduced by relaxation if the matrix has a low viscosity at the sintering temperature (glass or liquid phase sintering systems with a high amount of liquid) or by application of an external pressure (hot isostatic pressing (HIP), hot pressing (HP) or spark plasma sintering (SPS)). Nevertheless, the maximum amount of the hard component in the composite material is limited due to these effects. Nearly dense materials could only be achieved with about 30 vol.% of the c-BN or diamond inclusions (diamond/WC; cBN–Si_3N_4[6]). The volume content of the hard phase can be increased if the inclusions are partially solved in the matrix. However, this requires that the dissolved component (e.g. carbon) reacts with the matrix to prevent the precipitation of the thermodynamically metastable modification.

Another option is to use reactive sintering without shrinkage. In this case a strong skeleton of the hard particles can be formed in the green body. Contents of 50–70 vol.% can be reached. A possible application of this concept is the silicon infiltration of diamond, which is similarly conducted such as the Si–SiC production. As it was shown previously,[7,10] diamond is well wetted by liquid silicon at temperatures above 1450 °C, which enables pressureless infiltration. Such materials are produced under high pressure with 80–90 vol.% diamond.[8] It was shown that such type of materials can also be produced at normal pressure.[9–11] The process is schematically shown in Fig. 1. Therewith, a hardness of up to 3400 HV and a fracture toughness of 5 MPa $m^{1/2}$ were achieved,[12] indicating the high potential of this material. The reaction of diamond with the infiltrating Si is connected with a strong volume expansion of the solid phase (volume increase of 266% in relation to the volume of the diamond). Formed SiC grows into pores without changing the outer dimensions of the components. Consequently, SiC can block the pore channels and prevent further infiltration. Similar behavior was found for the SiC materials produced from carbon in wood-based systems.[13] Our previous work showed that infiltration is possible if the grain size of diamond is larger than 10–20 μm.[10,11] For smaller grain sizes, the maximum infiltration depths of 2–3 mm were achieved. Therefore, SiC–diamond materials with low diamond grain sizes can be prepared only as graded or layered materials with a diamond–silicon carbide layer having the thickness of 1–3 mm on a Si-infiltrated SiC substrate. This results in an advantage of such materials due to the ability for smaller diamond grain sizes to be used and for the wear properties of the materials to be tailored. Such a layered or graded material also exhibits a cost advantage due to the lower raw material and finishing costs involved in its production. Up to now, the preparation of such layered materials has not been realized. The paper examines the possibility of preparing these materials and comparing them with non-graded materials. An emphasis is put on the microstructure formation because no detailed data are available.

2. Experimental

2.1. Preparation of the materials

Preforms for the infiltration with silicon were produced alternatively by casting or pressing a mixture of diamond powder (Element Six (Pty) Ltd.) and phenolic resin (Hexion Ltd.). The diamond powder had the average grain size of 10 μm. The 10 μm powder was chosen because this grain size allows a directly comparison between graded and the non-graded materials.

For casting of the green body, a slurry containing a dispersion of the diamond powder and a liquid phenolic resin (25.4 wt.%) was prepared. After shaping the binder was crosslinked by heat treatment in furnace up to 180 °C in air.

For pressing, 9 wt.% of solid phenolic resin was dissolved in ethanol and mixed with the diamond powder. The slurry was dried using a rotary evaporator; the resulting powder was screened at 212 μm and compacted at a pressure of 40 MPa. For preparation of a graded green compact, a two-step pressing technique was used by pressing Si–SiC granulate material (substrate material) in a first step and the diamond material on top of the substrate layer in a second step. The crosslinking was achieved by heat treatment up to a temperature of 180 °C in air. The preforms obtained using both methods were then pyrolysed in argon up to a temperature of 900 °C. Subsequently, liquid silicon infiltration was carried out using a FAST/SPS-furnace (HP D25 FCT, Germany) equipped with a furnace cartridge tool instead of the normal uniaxial pressing tools. The crucible tool was loaded with the green body and with coarse-grained silicon powder. The setup was heated in a vacuum at a heating rate of 50 K/min up to the infiltration temperatures of 1550 °C, 1600 °C and 1650 °C, respectively.

2.2. Methods of characterization

For microstructural characterization the infiltrated materials were cut by a laser beam; the cross sections of the samples were polished using a broad ion beam technique. Phase microstructures, morphologies, compositions and orientations were investigated using a scanning electron microscope NVision 40 (Carl Zeiss SMT GmbH) that was equipped with a field emission cathode (FESEM), an energy dispersive detector of characteristic X-rays (EDX) and with an Oxford Instruments Ltd. NordlysS EBSD detector (Oxford Instruments Ltd. NordlysS) for registration of the electron back-scatter diffraction

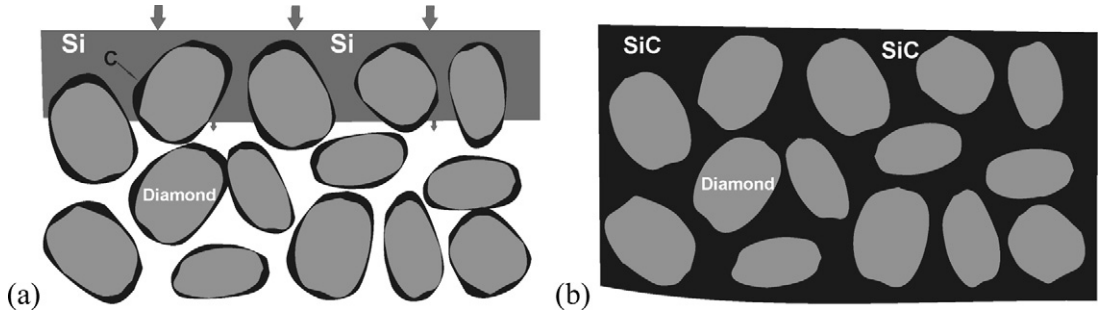

Fig. 1. Schematic representation of the liquid silicon infiltration of a preform beginning of the infiltration and (b) after infiltration.

Table 1
Phase composition determined by XRD and hardness of the composites.

Material name	Infiltration temperature [°C]	Phase content [vol.%]				Hardness [GPa]
		SiC	Diamond	Graphite	Silicon	
Nongraded						
GC_1550	1550	47.8 ± 0.7	51.2 ± 1.2	–	1.0 ± 0.1	48.6 ± 1.6
GC_1600	1600	49.1 ± 0.6	49.6 ± 1.0	0.4 ± 0.1	0.9 ± 0.1	29.8 ± 2.2
GC_1650	1650	49.9 ± 0.5	44.8 ± 0.9	5.3 ± 0.6	–	17.5 ± 2.4
Layered[a]						
P0034	1550	49.7 ± 1.0	45.8 ± 2.1	–	4.5 ± 1.0	–

[a] Phase composition of the diamond–SiC surface layer.

(EBSD) patterns. For the determination of the phase compositions an ID 3003 Theta/Theta X-ray diffractometer (GE Inspection Technologies) with a CuKα source and an energy-dispersive detector (Roentec) was used. The X-ray diffraction (XRD) patterns were measured in the range of the diffraction angles from 10° to 120° with the step size of 0.02°.

Raman spectra were recorded using a Horiba Scientific Ltd. LabRAM HR Raman microimaging system. The laser wavelength was 473 nm with a laser spot size of 0.85 μm at a radiation power of ~2000 kW/cm^2. The calibration was done using a silicon single crystal (520 cm^{-1}), the confocal hole was 1000 μm, the slit 100 μm, the exposure time ranged between 5 s and 15 s.

The Knoop hardness was measured on an XM 1280 from Ahotec Ltd.; the load applied to the indenter was 19.6 kN.

The thermodynamic calculations were carried out using the Factsage programme[14] and the data determined by Groebner.[15]

3. Results

The labeling of the prepared samples and their main characteristics are given in Table 1. All materials under study were fully infiltrated regardless of the infiltration temperature. A typical microstructure is shown in the micrographs in Fig. 2. Diamond, SiC and Si are clearly visible in Fig. 2a. The micrograph in Fig. 2b reveals that the amount of silicon can be significantly reduced in the diamond–SiC layer (no Si visible in Fig. 2b). The lack of residual porosity indicates the successful infiltration. SiC grains with different sizes are formed. Large platelet-like SiC crystals formed on the surface of the diamond beside sub-μm to nm-sized SiC crystals also formed (Fig. 3). The large facetted

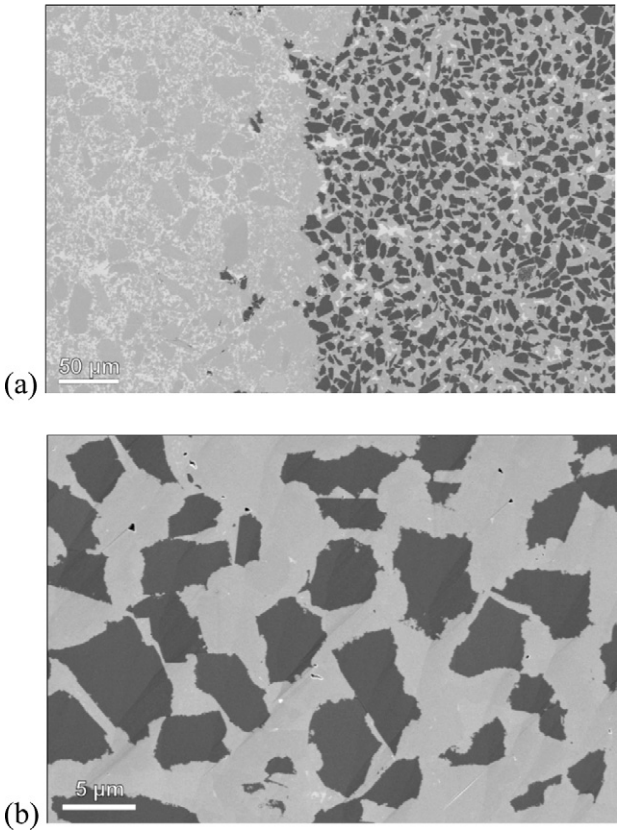

Fig. 2. FESEM micrographs of the diamond–SiC composite P0034 (a) interface between the substrate (left) and the diamond composite layer (right), (b) microstructure of the diamond/SiC-composite taken at a higher magnification (the black particles are diamond, the gray is SiC and the white is silicon).

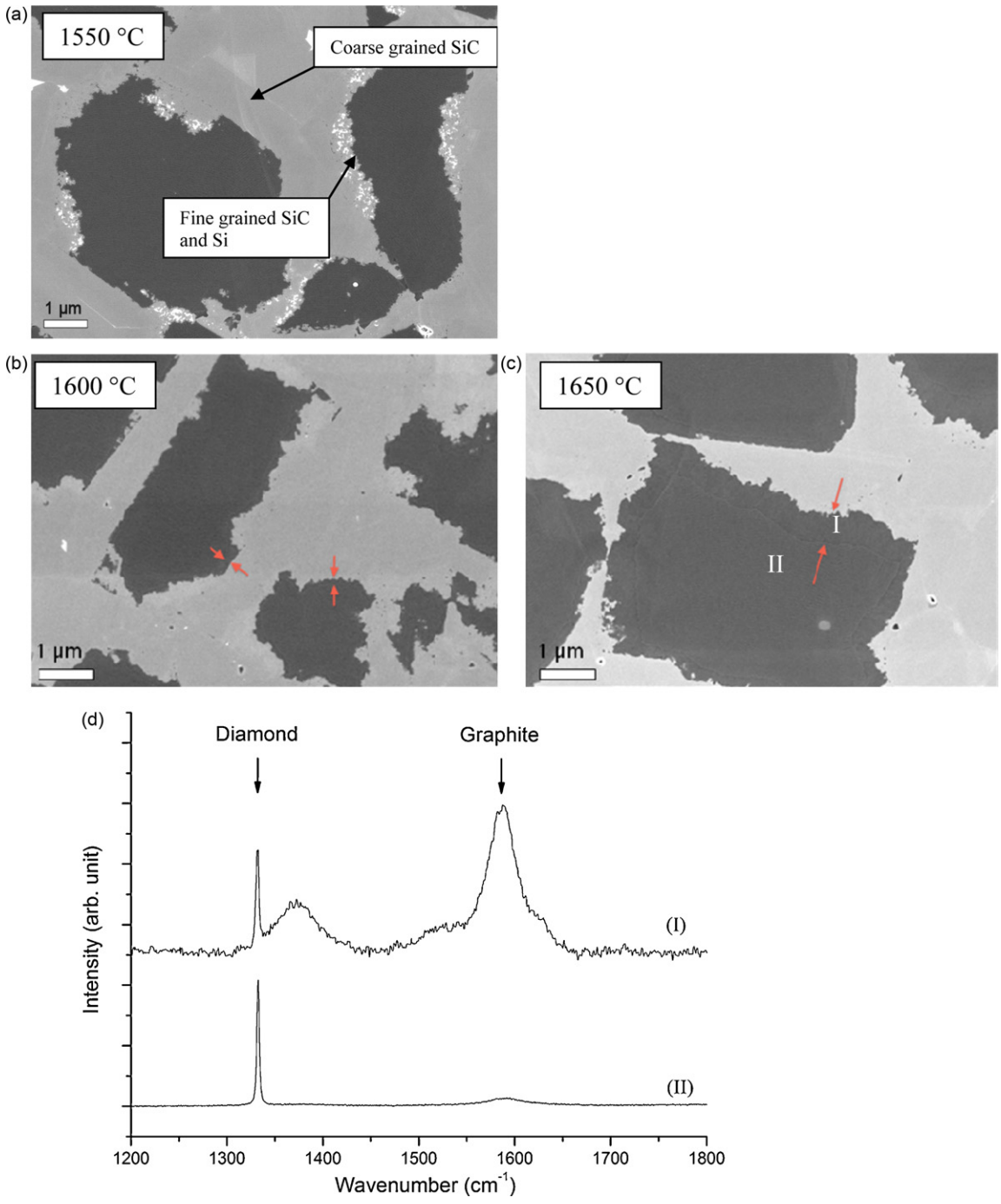

Fig. 3. Microstructure of the materials infiltrated at temperatures of 1550 °C (a), 1600 °C (b) and 1650 °C (c). The graphite layers on the surface of the diamond particles in the materials infiltrated at temperatures of 1600 and 1650 °C are marked by arrows. (d) The Raman spectra are given measured in the marked areas in (c).

crystals are often located on the flat crystal surfaces, whereas the smaller crystals formed on rough interfaces. In these areas remaining nanocrystalline silicon can also be found (bright dots in Fig. 3a). The orientation of the larger SiC crystals in relation to the diamond particles was investigated by EBSD. Many SiC crystals were found to exhibit a relationship between their orientation and that of the neighbouring diamond grains (Fig. 4). It was shown that an orientation relationship between diamond and β-SiC exists in materials prepared by infiltration of pure diamonds.[16]

Diamond, cubic β-SiC (polytype 3C) and silicon as the dominant crystalline phases in the infiltrated samples were identified using X-ray diffraction (Fig. 5). In the samples densified at temperatures of 1600 °C and 1650 °C, a weak reflection maximum appeared at 2Θ of 26.8 in the XRD-pattern which can be attributed to graphite that formed during the partial transformation of diamond at higher infiltration temperatures. FESEM micrographs indicate that the graphite is located at the diamond/SiC interfaces (Fig. 3). Partial graphitization of diamond at the interfaces to SiC was confirmed by HRTEM[17] and Raman

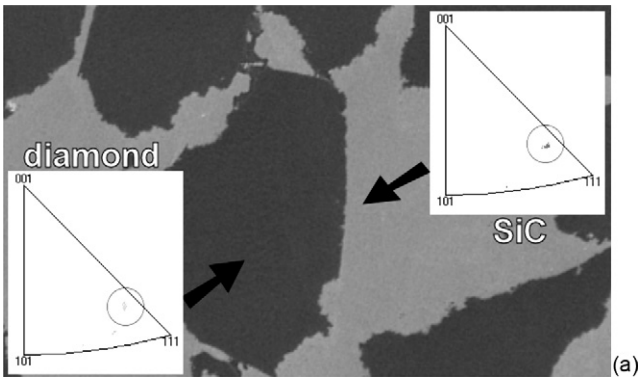

Fig. 4. EBSD pole figures of the orientation relationship between diamond and SiC–3C (a) and FESEM micrograph showing the growth of large SiC grains on the surface (b).

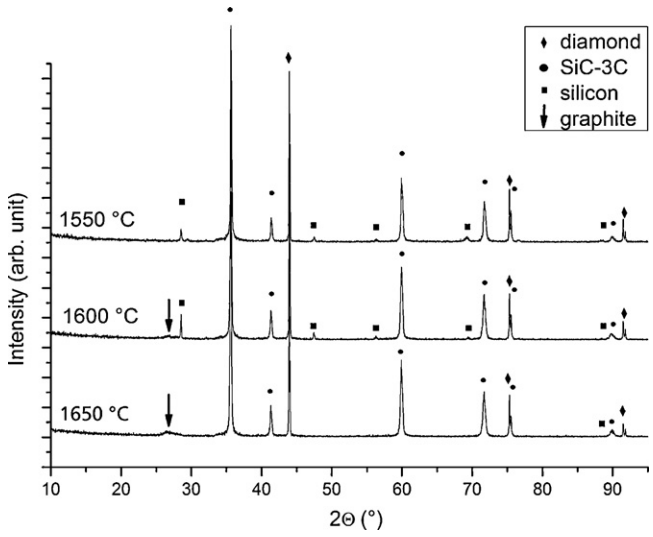

Fig. 5. XRD pattern of the materials infiltrated at temperatures of 1550 °C, 1600 °C and 1650 °C.

spectroscopy. On the contrary, no graphite could be detected in the material infiltrated at a temperature of 1550 °C in XRD, FESEM and HRTEM measurements (see Figs. 3 and 5). The contents of phases summarized in Table 1 were determined using the Rietveld analysis (software: AutoQuan; GE Inspection Technology). The diamond content in the material was around 50 vol.%. It decreased slightly with increasing infiltration temperature due to partial graphitization. XRD patterns revealed a reduction in silicon content with increasing infiltration temperature (Fig. 5 and Table 1). Additionally, the phase composition was determined using image analysis of the FESEM micrographs. These results are in agreement with the phase composition determined by the Rietveld analysis. For example 48.0 ± 1.0 vol.% diamond was determined by image analysis and 45.8 ± 2.1 vol.% by XRD in the diamond–SiC surface of the layered composite (P0034).

The micro Raman spectroscopy investigations confirmed the presence of Si, SiC and diamond in the samples. Raman spectra of the sample infiltrated at a temperature of 1600 °C exhibited a carbon G-mode. A detailed analysis of the Raman spectra in the wavenumber range between 720 cm^{-1} and 820 cm^{-1} revealed the presence of several SiC polytypes (3C, 4H, 6H) (Fig. 6b) and additionally sharp but shifted modes of β-SiC (3C) (Fig. 6a). Also, the silicon peaks were strongly shifted in comparison to the measured silicon standard ($\Delta\omega = 5.6 \pm 0.2\ cm^{-1}$). The strong shifts of silicon and silicon carbide modes were due to internal stresses in the material. The silicon modes shifted to higher wave numbers, whereas the β-SiC peaks shifted to lower wave numbers ($\Delta\omega_{max} = 1.5\ cm^{-1}$), indicating that silicon was under compressive stress whereas β-SiC was under tensile stress. A residual compressive stress in silicon was estimated to be about −1.17 GPa using Eq. (1).[18]

$$\sigma_{Si} = -0.209 \cdot \Delta\omega_{Si} \quad (1)$$

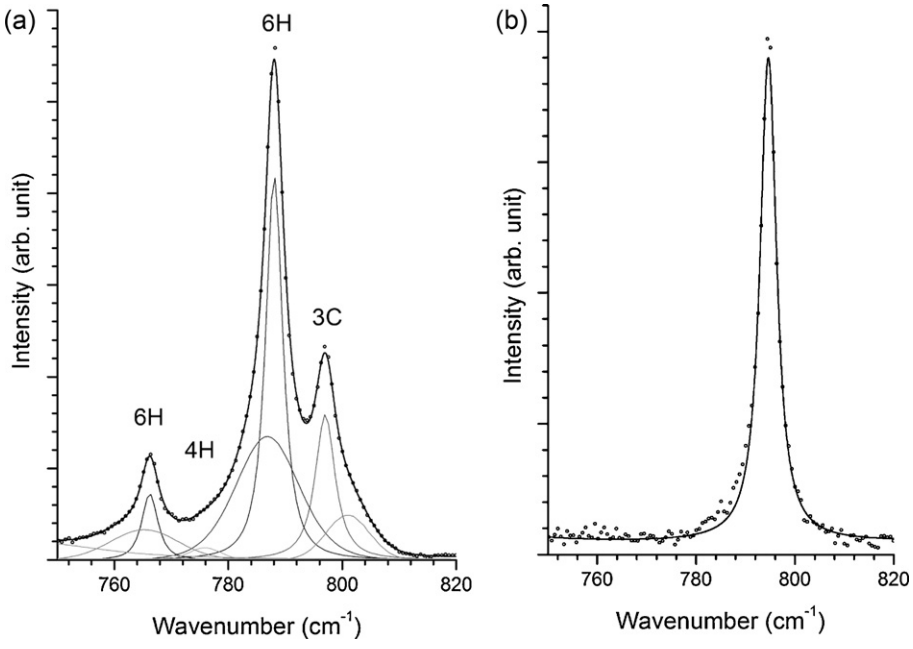

Fig. 6. Raman spectra taken at different positions within the silicon carbide grains.

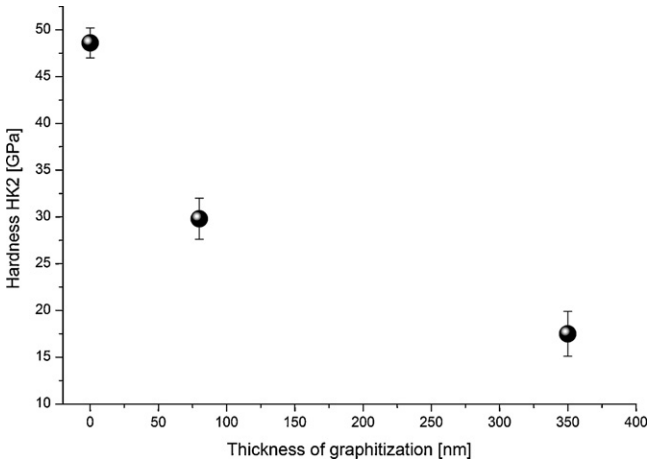

Fig. 7. Measured hardness as a function of the thickness of the graphite layer that formed at the diamond surface.

In Fig. 7 the measured hardness as a function of the graphite layer at the surface of the diamond is given. A hardness value of 47 GPa (HK2) was determined for the material infiltrated at a temperature 1550 °C. The hardness depends strongly on the amount of graphite. With increasing thickness of the graphite layer the interface between diamond and matrix becomes weaker and the hardness drops to values as low as 17.5 GPa. Therefore the infiltration has to be carried out in such a way, that the graphitization of the diamond can be avoided.

4. Discussion

4.1. Microstructure formation

General features of the microstructure formation derived of previous investigations[7,16] and results of this work are exhibited schematically in Fig. 8. During infiltration, the liquid silicon reacts both with the remaining carbon from the resin and with the diamond by forming SiC. No residual non-diamond carbon (graphite or amorphous carbon from the resin) is observed in the materials infiltrated at temperatures of 1550 °C. Thus all remaining carbon of the added resin reacts with the Si, reducing the consumption of diamond during the infiltration.

The orientation relationships determined using EBSD between the diamond and the SiC formed reveal that nucleation

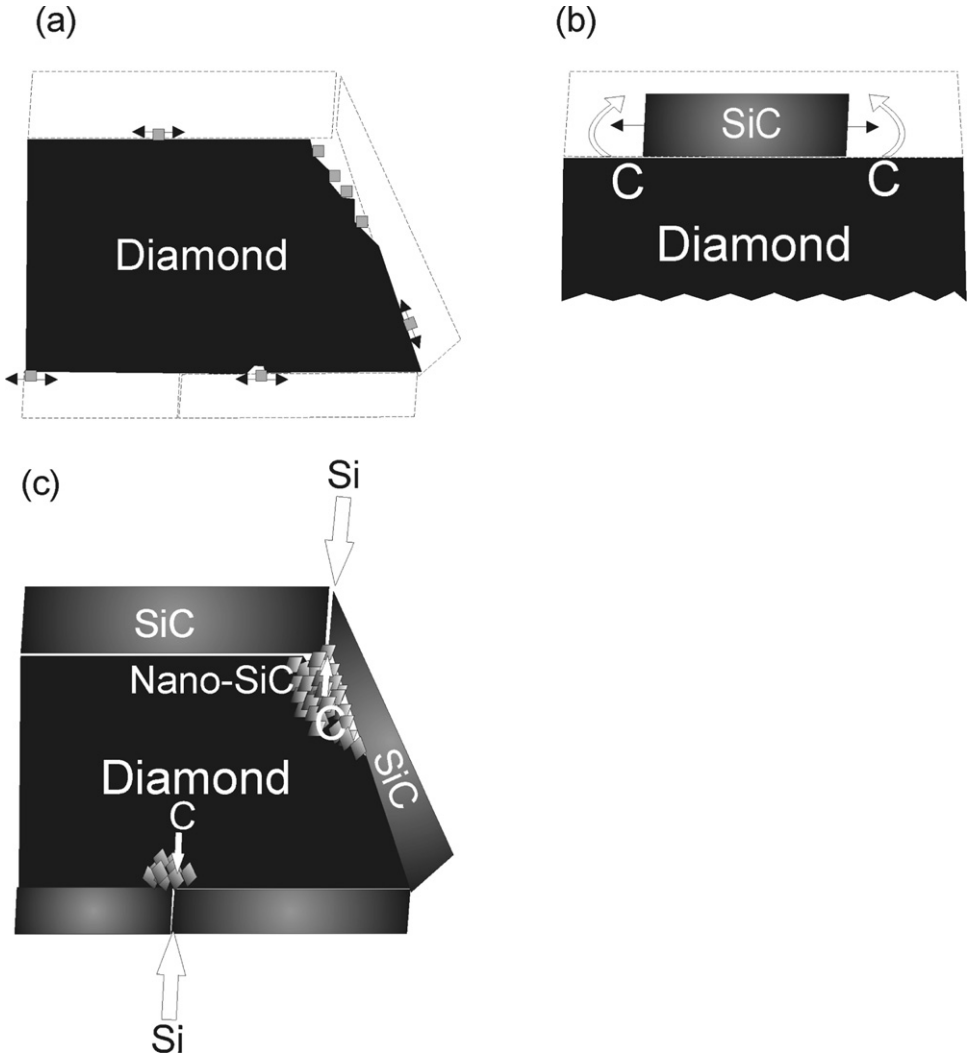

Fig. 8. Formation mechanism of SiC with different morphologies.

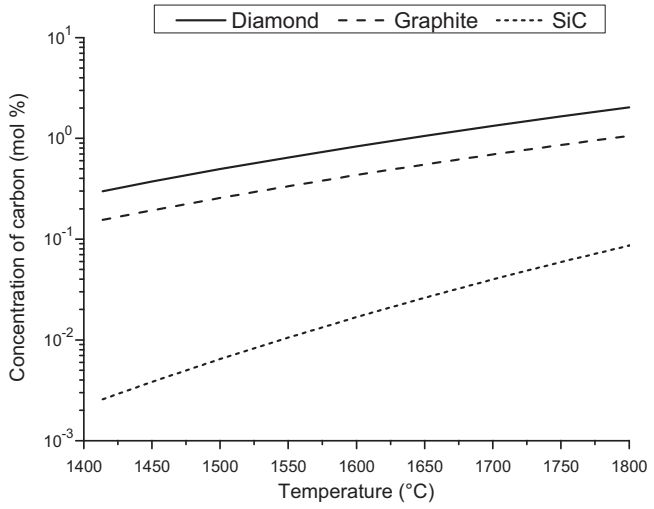

Fig. 9. Calculated equilibrium concentrations of carbon in liquid silicon saturated with regard to diamond, graphite and SiC.

takes place mostly on the surfaces of the diamond grains. Nucleation on the well-facetted grains is a slow process and hence large platelet like grains are formed. This explains the formation of the large grains at the interface in our investigations and was also observed by the interaction of CVD diamond with silicon.[7]

These platelet-like SiC grains grow fast. It can be assumed that this reaction involves transport through the liquid phase. An explanation for this transport mechanism can be deduced by taking the solubility of carbon in silicon into account (Fig. 9). Approximately 1 mol.% carbon can be dissolved in liquid silicon at infiltration temperatures between 1550 and 1600 °C before the saturation with carbon is reached. The saturation occurs at the interface between the direct contact of diamond and liquid silicon. The equilibrium carbon concentration in liquid silicon in contact with SiC is only 0.01 mol.%. The strong concentration gradients of carbon which exists in the melt between the area of dissolution of carbon and growing SiC are responsible for the carbon transport via the liquid phase.

On the non-facetted surfaces of the diamond (formed by crushing of the diamond during production) finer SiC crystals are formed indicating the more pronounced nucleation.

Investigations of the reaction of liquid silicon with CVD diamond, glassy carbon and graphite[19,20] have shown that in all cases the reaction results in very fast formation of a protective SiC layer around the diamond grains. After the formation of the protective layer, the reaction rate strongly decreases.[7,20] This is because of the very low diffusion coefficients of Si and C in the crystal lattice of SiC.[21,22] Further reaction between Si and C is controlled by diffusion along the grain boundaries in the SiC layers due to the higher diffusion coefficients at the grain boundary. An inward diffusion of Si and an outward diffusion of C must exist (Fig. 8c). At this stage, most of the small SiC-nanocrystals must be formed. This is in agreement with the data found under conditions for the formation of nanocrystalline SiC in biomorphic SiC.[13]

Infiltration at temperatures between 1650 °C and 1600 °C leads to the formation of a graphite-like layer on the surface of the diamond grains. This indicates that the temperature during infiltration exceeds the stability range of the diamond. It has to be mentioned, that diamond starts to transform into graphite predominantly at the surface or at internal defects.[23] Because this layer is found between the diamond and the SiC, it is assumed that it is formed after the infiltration has started; otherwise it would be very likely that it would be dissolved in silicon. Since the reaction of carbon with Si is strongly exothermic (ΔH (1500 °C) = −74.12 kJ/mol) the local temperature can be much higher than the nominal furnace temperature. This could be an additional reason for the start of the conversion of diamond into graphite. Consequently by adapting the heat treatment cycle the formation of graphite layers can be prevented and a silicon contents below 1 vol.% can be reached. The comparison of the microstructure of the layered and non-layered materials showed no differences if the same grain size of the diamond was used in both kinds of materials. Cracks or segregations of silicon at the boundary between the diamond containing layer and the Si infiltrated substrate were not observed despite the stresses which could be expected at the interface.

Table 2
Thermal expansion coefficient, Young's moduli and Poisson's ratio of the phases used for the calculation.[2,24]

Component	Properties		
	Thermal expansion (1/K)	Young's modulus (GPa)	Poisson's ratio
Silicon	4.5×10^{-6}	169	0.279
Silicon carbide	4.5×10^{-6}	450	0.212
Diamond	5.0×10^{-6}	1050	0.144

4.2. Internal stresses and properties

In composite materials comprising components with different thermal expansion coefficients local internal stresses occur. Isolated inclusions in a matrix having higher thermal expansion coefficient in comparison to the matrix are under hydrostatic tensile stresses. The surrounding matrix exhibit tangential compressive stresses and radial tensile stresses. If they are too high in comparison to the strength of the material the stresses can relax by micro crack formation at the interface between particle and matrix. If the thermal expansion coefficient of the inclusion is lower than that of the matrix the inclusion is under compressive stress and the surrounding matrix exhibit tensile tangential and compressive radial stresses.

Assuming spherical inclusions (diamond in the SiC matrix) the stress at the interface diamond–SiC can be calculated.[24] This is a commonly used, first approximation of the stresses and can be used to explain the stresses experimentally observed. The elastic properties of the components used for the calculations are summarized in Table 2.[1,25] Calculation of the stress regarding the interface between diamond and a SiC matrix at a temperature difference of 1400 °C implies that the radial stress at the interface diamond/SiC is a tensile stress and can reach a value of 340 MPa. While the diamond particles will be under hydrostatic tensile stress of 340 MPa.

Table 3
Calculated macroscopic stress between substrate (Si–SiC) and layer (diamond–SiC–Si) for different phase compositions and different sample geometries. For the calculations the composition of Si–SiC was assumed as 70 vol.% SiC and 30 vol.% Si. The composition of the top layer is varied and is given in the table (σ_{sub} – stress in the substrate; σ_{Dia} – stress in the diamond composite layer).

Composition of the diamond composite layer	Layer/substrate thickness	2 mm/5 mm	2 mm/7 mm	1 mm/5 mm	1 mm/7 mm
50 vol.% SiC	σ_{sub} [MPa]	−73	−60	−47	−36
50 vol.% diamond	σ_{Dia} [MPa]	183	209	233	253
60 vol.% SiC	σ_{sub} [MPa]	−60	−48	−38	−29
40 vol.% Diamond	σ_{Dia} [MPa]	149	169	188	203
55 vol.% SiC	σ_{sub} [MPa]	−78	−63	−49	−38
40 vol.% Diamond	σ_{Dia} [MPa]	196	222	246	266
5 vol.% Si					
50 vol.% SiC	σ_{sub} [MPa]	−85	−69	−54	−42
45 vol.% Diamond	σ_{Dia} [MPa]	213	242	269	291
5 vol.% Si					

Additionally, internal stresses are generated by silicon. It has the same coefficient of thermal expansion as SiC, but during solidification it expands by nearly 9 vol.%. If it forms a three-dimensional network this stress can be relaxed by squeezing out the silicon. If the silicon forms isolated inclusions then it will contribute to the internal stress. Thus, the solidified silicon particles are under compressive stresses.

The Raman measurements show strong shifts of the characteristic modes of Si and SiC in the composites indicating the compressive stress of silicon and the tensile stress in the SiC as predicted by the model. The hexagonal SiC polytypes observed by Raman measurements usually form only at temperatures above 1800 °C. The formation of the polytypes can be caused by reducing the stresses from the epitaxial growth or due to the internal stress. The observed fluctuations of the stress in the material are the reason for the relatively good toughness of these materials.

In the case of the layered or graded composite e.g. diamond/SiC top layer and the Si–SiC substrate as in the sample P0034 additional stresses are formed between the layers superimposing the local stresses discussed before.[24]

The calculated stress values between the substrate (Si–SiC) and the layer (diamond–SiC–Si) for different phase compositions and different sample geometries are given in Table 3. From these results can be concluded that the surface layer is under tensile stress in the range of 150–290 MPa. This weakens the surface of the material slightly but does not result in delamination of the layers. The stress reduces with the increasing ratio of the thickness of the surface layer to the substrate thickness and only slightly changes with the diamond/SiC ratio.

5. Conclusions

SiC-bonded diamond prepared by pressureless infiltration of diamond preforms represents a promising new class of materials with strongly improved wear behavior in comparison to hard metal and ceramics. It allows cost-effective pressureless preparation of a ultrahard SiC–diamond composite with approximately 50 vol.% diamond. The material can be graded or nongraded depending on the given application.

These materials are harder than conventional c-BN based materials exhibiting hardness values of 30–40 GPa.[26]

References

1. Riedel R. *Ceramic hard materials*. Wiley-VCH Verlag GmbH & Co. KG; 2000.
2. Schäfer L. *Diamantbeschichtete Keramik DiaCer: Leistungsfähiger Werkstoffverbund für extreme Anforderungen*. Diamond Business; 2011. p. 22–6.
3. Matthey T, Schrüfer A. *CVD Diamantinnovation setzt sich durch*. Diamond Business; 2011. p. 6–9.
4. www.eagleburgmann.com.
5. Rahaman MN. *Ceramic processing and sintering*. New York: Marcel Dekker Inc.; 2005.
6. Ye F, Zhaoping H, Zhang H, Liu L, Zhou Y. Spark plasma sintering of cBN/-SiAlON composites. *Mater Sci Eng A* 2010;**527**:4723–6.
7. Mlungwane K, Sigalas I, Herrmann M, Rodrıguez M. The wetting behaviour and reaction kinetics in diamond–silicon carbide systems. *Ceram Int* 2009;**35**:2435–41.
8. Ko YS, Tsurumi T, Fukunaga O, Yano T. High pressure sintering of diamond-SiC composite. *J Mater Sci* 2001;**36**:469–75.
9. Gordeev S, Zhukov S, Danchukova L, Ekström T. Method of manufacturing a diamond–silicon carbide–silicon composite and a composite produced by this method. US patent, 709,747; 2004.
10. Mlungwane K, Sigalas I, Herrmann M. Development of a diamond silicon carbide composite material, Industriediamantenrundschau 2006;**40**:20–4.
11. Mlungwane K, Sigalas I, Herrmann M. The low-pressure infiltration of diamond by silicon to form diamond-silicon carbide composites. *J Eur Ceram Soc* 2008;**28**:321–6.
12. http://www.e6.com/en/businessareas/e6hardmaterials/siliconcemented diamondcompositescd/.
13. Zollfrank C, Sieber H. Microstructure evolution and reaction mechanism of biomorphic SiSiC ceramics. *J Am Ceram Soc* 2005;**88**:51–8.
14. Bale CW, Chartrand P, Degterov SA, Eriksson G, Hack K, Ben Mahfoud R, et al. FactSage thermochemical software and databases. *Calphad* 2002;**26**:189–228.
15. Groebner J. Constitution calculations in the system Y–Al–Si–C–O. Ph.D. thesis, University of Stuttgart, Germany, database: 1994.9288A00S—SGTE Si-Y-Al-C-O Database. Scientific Group Thermodata, Europe; 2000.
16. Park JS, Sinclair R, Rowcliff D, Stern M, Davidson H. Orientation relationship in diamond and silicon carbide composites. *Diamond Relat Mater* 2007;**16**:562–5.
17. Muehle U, Leuteritz A, Matthey B, Hermann M, Chmelik D, Seifert H.-J, Rafaja D. FIB-based preparation of phase boundaries in diamond reinforced ceramics for HR- and analytical TEM investigations, FIB-workshop 27./28.6 2011, Zürich.

18. De Wolf I. Micro-Raman spectroscopy to study local mechanical stress in silicon integrated circuits. *Semicond Sci Technol* 1996;**11**:139–54.
19. Sangsuwan P, Tewari SN, Gatica JE, Singh M, Dickerson R. Reactive infiltration of silicon melt through microporous amorphous carbon preforms. *Metall Mater Trans B* 1999;**30B**:933.
20. Zhou H, Singh RN. Kinetics model for the growth of silicon carbide by the reaction of liquid silicon with carbon. *J Am Ceram Soc* 1995;**78**: 2456–62.
21. Hon MH, Davis RF. Self-diffusion of ^{14}C in polycrystalline β-SiC. *J Mater Sci* 1979;**14**:2411–21.
22. Hon MH, Davis RF, Newbury DE. Self-diffusion of ^{30}Si in polycrystalline β-SiC. *J Mater Sci* 1980;**15**:2073–80.
23. Pantea C, Qian J, Voronin GA, Zerda TW. High pressure study of graphitization of diamond crystals. *J Appl Phys* 2002;**91**:1957–62.
24. Salmang H, Scholze H. *Keramik*. Berlin: Springer; 2006. p. 392–3.
25. Landolt HH, Börnstein R. *Landolt-Börnstein-Tabellenwerk Zahlenwerte und Funktionen aus Naturwissenschaft und Technik*. Heidelberg: Landolt Springer-Verlag; 1961.
26. McKie A, Winzer J, Sigalas I, Herrmann M, Weiler L, Rödel J, et al. Mechanical properties of cBN–Al composite materials. *Ceram Int* 2011;**37**:1–8.